EUROPEAN LABORATORY FOR PARTICLE PHYSICS

CERN-EP/98-039
6th March 1998

Search for Stable and Long-Lived Massive Charged Particles in e^+e^- Collisions at $\sqrt{s} = 130 - 183$ GeV

The OPAL Collaboration

Abstract

A search for stable and long-lived massive particles of electric charge $|Q/e| = 1$ or 2/3, pair-produced in e^+e^- collisions at centre-of-mass energies from 130 to 183 GeV, is reported by the OPAL collaboration at LEP. No evidence for production of these particles was observed in a mass range between 45 and 89.5 GeV. Model-independent upper limits on the production cross-section between 0.05 and 0.19 pb have been derived for scalar and spin-1/2 particles with charge ± 1. Within the framework of the minimal supersymmetric model (MSSM), this implies a lower limit of 82.5 (83.5) GeV on the mass of long-lived right- (left-)handed scalar muons and scalar taus. Long-lived charged leptons and charginos are excluded for masses below 89.5 GeV. For particles with charge $\pm 2/3$ the upper limits on the production cross-section vary between 0.05 and 0.2 pb. All limits, on masses and on cross-sections, are valid at the 95% confidence level for particles with lifetimes longer than 10^{-6} s.

(Submitted to Physics Letters B)

The OPAL Collaboration

K. Ackerstaff[8], G. Alexander[23], J. Allison[16], N. Altekamp[5], K.J. Anderson[9], S. Anderson[12], S. Arcelli[2], S. Asai[24], S.F. Ashby[1], D. Axen[29], G. Azuelos[18,a], A.H. Ball[17], E. Barberio[8], R.J. Barlow[16], R. Bartoldus[3], J.R. Batley[5], S. Baumann[3], J. Bechtluft[14], T. Behnke[8], K.W. Bell[20], G. Bella[23], S. Bentvelsen[8], S. Bethke[14], S. Betts[15], O. Biebel[14], A. Biguzzi[5], S.D. Bird[16], V. Blobel[27], I.J. Bloodworth[1], M. Bobinski[10], P. Bock[11], D. Bonacorsi[2], M. Boutemeur[34], S. Braibant[8], L. Brigliadori[2], R.M. Brown[20], H.J. Burckhart[8], C. Burgard[8], R. Bürgin[10], P. Capiluppi[2], R.K. Carnegie[6], A.A. Carter[13], J.R. Carter[5], C.Y. Chang[17], D.G. Charlton[1,b], D. Chrisman[4], P.E.L. Clarke[15], I. Cohen[23], J.E. Conboy[15], O.C. Cooke[8], C. Couyoumtzelis[13], R.L. Coxe[9], M. Cuffiani[2], S. Dado[22], C. Dallapiccola[17], G.M. Dallavalle[2], R. Davis[30], S. De Jong[12], L.A. del Pozo[4], A. de Roeck[8], K. Desch[8], B. Dienes[33,d], M.S. Dixit[7], M. Doucet[18], E. Duchovni[26], G. Duckeck[34], I.P. Duerdoth[16], D. Eatough[16], P.G. Estabrooks[6], E. Etzion[23], H.G. Evans[9], M. Evans[13], F. Fabbri[2], A. Fanfani[2], M. Fanti[2], A.A. Faust[30], L. Feld[8], F. Fiedler[27], M. Fierro[2], H.M. Fischer[3], I. Fleck[8], R. Folman[26], D.G. Fong[17], M. Foucher[17], A. Fürtjes[8], D.I. Futyan[16], P. Gagnon[7], J.W. Gary[4], J. Gascon[18], S.M. Gascon-Shotkin[17], N.I. Geddes[20], C. Geich-Gimbel[3], T. Geralis[20], G. Giacomelli[2], P. Giacomelli[4], R. Giacomelli[2], V. Gibson[5], W.R. Gibson[13], D.M. Gingrich[30,a], D. Glenzinski[9], J. Goldberg[22], M.J. Goodrick[5], W. Gorn[4], C. Grandi[2], E. Gross[26], J. Grunhaus[23], M. Gruwé[27], C. Hajdu[32], G.G. Hanson[12], M. Hansroul[8], M. Hapke[13], C.K. Hargrove[7], P.A. Hart[9], C. Hartmann[3], M. Hauschild[8], C.M. Hawkes[5], R. Hawkings[27], R.J. Hemingway[6], M. Herndon[17], G. Herten[10], R.D. Heuer[8], M.D. Hildreth[8], J.C. Hill[5], S.J. Hillier[1], P.R. Hobson[25], A. Hocker[9], R.J. Homer[1], A.K. Honma[28,a], D. Horváth[32,c], K.R. Hossain[30], R. Howard[29], P. Hüntemeyer[27], D.E. Hutchcroft[5], P. Igo-Kemenes[11], D.C. Imrie[25], K. Ishii[24], A. Jawahery[17], P.W. Jeffreys[20], H. Jeremie[18], M. Jimack[1], A. Joly[18], C.R. Jones[5], M. Jones[6], U. Jost[11], P. Jovanovic[1], T.R. Junk[8], J. Kanzaki[24], D. Karlen[6], V. Kartvelishvili[16], K. Kawagoe[24], T. Kawamoto[24], P.I. Kayal[30], R.K. Keeler[28], R.G. Kellogg[17], B.W. Kennedy[20], J. Kirk[29], A. Klier[26], S. Kluth[8], T. Kobayashi[24], M. Kobel[10], D.S. Koetke[6], T.P. Kokott[3], M. Kolrep[10], S. Komamiya[24], R.V. Kowalewski[28], T. Kress[11], P. Krieger[6], J. von Krogh[11], P. Kyberd[13], G.D. Lafferty[16], R. Lahmann[17], W.P. Lai[19], D. Lanske[14], J. Lauber[15], S.R. Lautenschlager[31], I. Lawson[28], J.G. Layter[4], D. Lazic[22], A.M. Lee[31], E. Lefebvre[18], D. Lellouch[26], J. Letts[12], L. Levinson[26], B. List[8], S.L. Lloyd[13], F.K. Loebinger[16], G.D. Long[28], M.J. Losty[7], J. Ludwig[10], D. Lui[12], A. Macchiolo[2], A. Macpherson[30], M. Mannelli[8], S. Marcellini[2], C. Markopoulos[13], C. Markus[3], A.J. Martin[13], J.P. Martin[18], G. Martinez[17], T. Mashimo[24], P. Mättig[26], W.J. McDonald[30], J. McKenna[29], E.A. Mckigney[15], T.J. McMahon[1], R.A. McPherson[28], F. Meijers[8], S. Menke[3], F.S. Merritt[9], H. Mes[7], J. Meyer[27], A. Michelini[2], S. Mihara[24], G. Mikenberg[26], D.J. Miller[15], A. Mincer[22,e], R. Mir[26], W. Mohr[10], A. Montanari[2], T. Mori[24], K. Nagai[26], I. Nakamura[24], H.A. Neal[12], B. Nellen[3], R. Nisius[8], S.W. O'Neale[1], F.G. Oakham[7], F. Odorici[2], H.O. Ogren[12], A. Oh[27], N.J. Oldershaw[16], M.J. Oreglia[9], S. Orito[24], J. Pálinkás[33,d], G. Pásztor[32], J.R. Pater[16], G.N. Patrick[20], J. Patt[10], R. Perez-Ochoa[8], S. Petzold[27], P. Pfeifenschneider[14], J.E. Pilcher[9], J. Pinfold[30], D.E. Plane[8], P. Poffenberger[28], B. Poli[2], A. Posthaus[3], C. Rembser[8], S. Robertson[28], S.A. Robins[22], N. Rodning[30], J.M. Roney[28], A. Rooke[15], A.M. Rossi[2], P. Routenburg[30], Y. Rozen[22], K. Runge[10], O. Runolfsson[8], U. Ruppel[14], D.R. Rust[12], K. Sachs[10], T. Saeki[24], O. Sahr[34], W.M. Sang[25], E.K.G. Sarkisyan[23], C. Sbarra[29], A.D. Schaile[34], O. Schaile[34], F. Scharf[3], P. Scharff-Hansen[8], J. Schieck[11], P. Schleper[11], B. Schmitt[8], S. Schmitt[11], A. Schöning[8], M. Schröder[8], M. Schumacher[3], C. Schwick[8], W.G. Scott[20],

T.G. Shears[8], B.C. Shen[4], C.H. Shepherd-Themistocleous[8], P. Sherwood[15], G.P. Siroli[2], A. Sittler[27], A. Skillman[15], A. Skuja[17], A.M. Smith[8], G.A. Snow[17], R. Sobie[28], S. Söldner-Rembold[10], R.W. Springer[30], M. Sproston[20], K. Stephens[16], J. Steuerer[27], B. Stockhausen[3], K. Stoll[10], D. Strom[19], R. Ströhmer[34], P. Szymanski[20], R. Tafirout[18], S.D. Talbot[1], P. Taras[18], S. Tarem[22], R. Teuscher[8], M. Thiergen[10], M.A. Thomson[8], E. von Törne[3], E. Torrence[8], S. Towers[6], I. Trigger[18], Z. Trócsányi[33], E. Tsur[23], A.S. Turcot[9], M.F. Turner-Watson[8], I. Ueda[24], P. Utzat[11], R. Van Kooten[12], P. Vannerem[10], M. Verzocchi[10], P. Vikas[18], E.H. Vokurka[16], H. Voss[3], F. Wäckerle[10], A. Wagner[27], C.P. Ward[5], D.R. Ward[5], P.M. Watkins[1], A.T. Watson[1], N.K. Watson[1], P.S. Wells[8], N. Wermes[3], J.S. White[28], G.W. Wilson[27], J.A. Wilson[1], T.R. Wyatt[16], S. Yamashita[24], G. Yekutieli[26], V. Zacek[18], D. Zer-Zion[8]

[1]School of Physics and Astronomy, University of Birmingham, Birmingham B15 2TT, UK
[2]Dipartimento di Fisica dell' Università di Bologna and INFN, I-40126 Bologna, Italy
[3]Physikalisches Institut, Universität Bonn, D-53115 Bonn, Germany
[4]Department of Physics, University of California, Riverside CA 92521, USA
[5]Cavendish Laboratory, Cambridge CB3 0HE, UK
[6]Ottawa-Carleton Institute for Physics, Department of Physics, Carleton University, Ottawa, Ontario K1S 5B6, Canada
[7]Centre for Research in Particle Physics, Carleton University, Ottawa, Ontario K1S 5B6, Canada
[8]CERN, European Organisation for Particle Physics, CH-1211 Geneva 23, Switzerland
[9]Enrico Fermi Institute and Department of Physics, University of Chicago, Chicago IL 60637, USA
[10]Fakultät für Physik, Albert Ludwigs Universität, D-79104 Freiburg, Germany
[11]Physikalisches Institut, Universität Heidelberg, D-69120 Heidelberg, Germany
[12]Indiana University, Department of Physics, Swain Hall West 117, Bloomington IN 47405, USA
[13]Queen Mary and Westfield College, University of London, London E1 4NS, UK
[14]Technische Hochschule Aachen, III Physikalisches Institut, Sommerfeldstrasse 26-28, D-52056 Aachen, Germany
[15]University College London, London WC1E 6BT, UK
[16]Department of Physics, Schuster Laboratory, The University, Manchester M13 9PL, UK
[17]Department of Physics, University of Maryland, College Park, MD 20742, USA
[18]Laboratoire de Physique Nucléaire, Université de Montréal, Montréal, Quebec H3C 3J7, Canada
[19]University of Oregon, Department of Physics, Eugene OR 97403, USA
[20]Rutherford Appleton Laboratory, Chilton, Didcot, Oxfordshire OX11 0QX, UK
[22]Department of Physics, Technion-Israel Institute of Technology, Haifa 32000, Israel
[23]Department of Physics and Astronomy, Tel Aviv University, Tel Aviv 69978, Israel
[24]International Centre for Elementary Particle Physics and Department of Physics, University of Tokyo, Tokyo 113, and Kobe University, Kobe 657, Japan
[25]Institute of Physical and Environmental Sciences, Brunel University, Uxbridge, Middlesex UB8 3PH, UK
[26]Particle Physics Department, Weizmann Institute of Science, Rehovot 76100, Israel
[27]Universität Hamburg/DESY, II Institut für Experimental Physik, Notkestrasse 85, D-22607

Hamburg, Germany
[28]University of Victoria, Department of Physics, P O Box 3055, Victoria BC V8W 3P6, Canada
[29]University of British Columbia, Department of Physics, Vancouver BC V6T 1Z1, Canada
[30]University of Alberta, Department of Physics, Edmonton AB T6G 2J1, Canada
[31]Duke University, Dept of Physics, Durham, NC 27708-0305, USA
[32]Research Institute for Particle and Nuclear Physics, H-1525 Budapest, P O Box 49, Hungary
[33]Institute of Nuclear Research, H-4001 Debrecen, P O Box 51, Hungary
[34]Ludwigs-Maximilians-Universität München, Sektion Physik, Am Coulombwall 1, D-85748 Garching, Germany

[a] and at TRIUMF, Vancouver, Canada V6T 2A3
[b] and Royal Society University Research Fellow
[c] and Institute of Nuclear Research, Debrecen, Hungary
[d] and Department of Experimental Physics, Lajos Kossuth University, Debrecen, Hungary
[e] and Department of Physics, New York University, NY 1003, USA

1 Introduction

Most searches for new particles predicted by models beyond the Standard Model (SM) assume that these particles decay promptly at the primary interaction vertex due to their very short lifetimes. These searches would not be sensitive to long-lived heavy particles which do not decay in the detectors. However several models predict such long-lived particles. For example, in the minimal supersymmetric model (MSSM) [1], if the mass difference between the chargino and the lightest neutralino is smaller than a few hundred MeV, the lightest chargino would have a lifetime sufficiently long to result in decays predominantly outside the detector. In gauge-mediated supersymmetry, if the slepton is the next-to-lightest supersymmetric particle, it could decay with a long lifetime to a lepton plus a goldstino, if the SUSY-breaking energy scale is sufficiently high [2]. R-parity violating SUSY models [3] also allow for long-lived heavy charged particles. If the lightest supersymmetric particle is a slepton and the R-parity violating coupling is small ($\lambda \leq 10^{-6}$), then the slepton decay length would be larger than a few meters, the typical size of tracking detectors at LEP. If a fourth-generation heavy lepton ($m_{\mathrm{L}} > m_{\mathrm{Z}}/2$) exists [4], the charged heavy lepton would be stable if it is lighter than its neutral isodoublet partner. Some models beyond the SM would also predict the existence of particles with fractional electric charge. As an example, leptoquarks [5] having a small coupling $\lambda_{\mathrm{L,R}}$ could be long-lived and possess fractional charge. Another example could be long-lived hadronic states with fractional charge predicted by some modified QCD models [6].

Previous searches for long-lived charged particles have been performed by the LEP collaborations with data taken at the Z^0 resonance [7]. The OPAL Limits on the production cross-section have been set at approximately 1.5 pb at 95% CL for masses between 34 and 44 GeV. DELPHI and ALEPH [8] have also analysed the data collected at centre-of-mass energies up to 172 GeV, setting limits of 0.2-0.4 pb for masses between 45 and 86 GeV.

This paper describes a search for long-lived particles $\mathrm{X}^{\pm}$, with $m_{\mathrm{X}} > m_{\mathrm{Z}}/2$, with charge $|Q/e| = 1$ or 2/3, pair-produced in the reaction $\mathrm{e^+e^-} \to \mathrm{X^+X^-}(\gamma)$. The data were collected by the OPAL detector during 1995-1997, at centre-of-mass energies of 130-136, 161, 172 and 183 GeV for a total integrated luminosity of 89.5 pb^{-1}. Such particles distinguish themselves by their anomalous, high or low ionization energy loss, $\mathrm{d}E/\mathrm{d}x$, in the tracking detector gas. This search is therefore primarily based on the precise $\mathrm{d}E/\mathrm{d}x$ measurement provided by the OPAL jet chamber. However, for particles of charge one, there is a large mass region where the measured $\mathrm{d}E/\mathrm{d}x$ cannot distinguish them from ordinary particles. A complementary search, based on the two-body kinematics, is used to cover this mass region. No search was made for particles with $|Q/e| = 1/3$ because their low ionization energy loss is too close to the jet chamber $\mathrm{d}E/\mathrm{d}x$ measurement threshold. The results obtained are valid for particles with a lifetime longer than 10^{-6} s.

2 The OPAL Detector

A complete description of the OPAL detector can be found in Ref. [9] and only a brief overview is given here. The central detector consists of a system of tracking chambers, providing charged particle reconstruction over 96% of the full solid angle[1] inside a 0.435 T uniform magnetic field

[1]The OPAL right-handed coordinate system is defined such that the z axis is in the direction of the electron beam, the x axis is horizontal and points towards the centre of the LEP ring, and θ and ϕ are the polar and

parallel to the beam axis. It consists of a two-layer silicon microstrip vertex detector, a high-precision drift chamber, a large-volume jet chamber and a set of z-chambers measuring the track coordinates along the beam direction.

The jet chamber (CJ) is the most important detector for this analysis. It is divided into 24 azimuthal sectors, each equipped with 159 sense wires. Up to 159 coordinate and $\mathrm{d}E/\mathrm{d}x$ measurements per track are thus possible, with a precision of $\sigma_{r\phi} \approx 135\,\mu$m and $\sigma_z \approx 6$ cm. When a track is matched with z-chamber hits the uncertainty on its z_0 coordinate is ≈ 1 mm. The jet and z-chambers, located inside the magnetic coil, provide a track momentum measurement with a resolution of $\sigma_p/p \approx \sqrt{(0.02)^2 + (0.0015 \cdot p_t)^2}$ for tracks with the full number of hits (p_t, in GeV, is the momentum transverse to the beam direction) and a resolution on the ionization energy loss measurement of approximately 2.8% for $\mu^+\mu^-$ events with a large number of usable hits for $\mathrm{d}E/\mathrm{d}x$ [10].

A lead-glass electromagnetic calorimeter (ECAL) located outside the magnet coil covers the full azimuthal range with excellent hermeticity in the polar angle range of $|\cos\theta| < 0.984$. The magnet return yoke is instrumented for hadron calorimetry (HCAL) covering the region $|\cos\theta| < 0.99$ and is followed by four layers of muon chambers. Electromagnetic calorimeters close to the beam axis complete the geometrical acceptance down to 24 mrad on both sides of the interaction point. These include the forward detectors (FD), which are lead-scintillator sandwich calorimeters and, at small angles, the silicon tungsten calorimeters (SW) [11]. The gap between the endcap ECAL and the FD is instrumented with an additional lead-scintillator electromagnetic calorimeter, called the gamma-catcher (GC).

The ionization energy loss $\mathrm{d}E/\mathrm{d}x$ produced by a charged particle is a function of $\beta\gamma = p/m$ and of the electric charge Q [10]. In Figure 1, the distribution of $\mathrm{d}E/\mathrm{d}x$ as a function of the apparent momentum, p/Q, is shown. Standard particles of charge ±1 (e, μ, π, p, K) with high momentum ($p > 0.1\sqrt{s}$ GeV) have $\mathrm{d}E/\mathrm{d}x$ between 9 and 11 keV/cm. Massive particles with charge ±1 are expected to yield $\mathrm{d}E/\mathrm{d}x > 11$ keV/cm for high-mass values, $m_{\mathrm{X}} > 0.36\sqrt{s}$ (e.g., at $\sqrt{s} = 183$ GeV, $m_{\mathrm{X}} = 65$ GeV, one has $p = 64$ GeV and $\mathrm{d}E/\mathrm{d}x = 11$ keV/cm), or $\mathrm{d}E/\mathrm{d}x < 9$ keV/cm for low-mass values, $m_{\mathrm{X}} < 0.27\sqrt{s}$ (e.g., at $\sqrt{s} = 183$ GeV, $m_{\mathrm{X}} = 50$ GeV, one has $p = 77$ GeV and $\mathrm{d}E/\mathrm{d}x = 8$ keV/cm). The $\mathrm{d}E/\mathrm{d}x$ measurement therefore provides a good tool for particle identification in this high- and low-mass regions. However, in the intermediate mass region, the $\mathrm{d}E/\mathrm{d}x$ measurement does not distinguish the signal from the background. In this region an analysis based on kinematic properties of pair-produced massive particles is used.

3 Monte Carlo Simulation

This section describes the Monte Carlo simulation of the signal and the background samples. All generated events have been processed through the full simulation of the OPAL detector [12]; the same event analysis chain has been applied to the simulated events and to the data.

To generate the signal process $\mathrm{e^+e^-} \to \mathrm{X^+X^-}(\gamma)$ different generators have been used. Signal events of the type $\mathrm{e^+e^-} \to \tilde{\ell}^+\tilde{\ell}^-(\gamma)$ ($\tilde{\ell}^\pm$ being a scalar lepton) have been generated at four different energies ($\sqrt{s} = 133, 161, 172, 183$ GeV) using SUSYGEN [13]. The generated scalar leptons are not allowed to decay, therefore simulating the signal from heavy charged stable

azimuthal angles, defined relative to the $+z$- and $+x$-axes, respectively. The radial coordinate is denoted by r.

scalar particles. Similarly, events of the type $e^+e^- \to L^+L^-(\gamma)$ and $e^+e^- \to Q\bar{Q}(\gamma)$, where $L^\pm$ are stable heavy leptons and Q, $\bar{Q}$ are stable heavy deconfined quarks with charge $\pm 2/3$, have been generated at the same energies, using the generator EXOTIC [14]. All signal samples have been generated with m_X ranging from 45 GeV to 90 GeV. Each sample contains 1000 events. For the purpose of detector simulation and particle interactions, $\tilde{\ell}^\pm$ and $L^\pm$ particles have been treated as heavy muons, while Q, $\bar{Q}$ as heavy stable hadrons with charge $\pm 2/3$.

The background has been estimated using simulations of all Standard Model processes (lepton-pair and multihadronic processes, four-fermion processes, two-photon processes). The Monte Carlo samples generated at $\sqrt{s} = 171$ and 184 GeV are briefly described below. Small differences in the centre-of-mass energies between data and the simulated background Monte Carlo samples have a negligible effect on the analysis. A detailed description of the Monte Carlo samples generated at $\sqrt{s} = 133$ GeV and $\sqrt{s} = 161$ GeV can be found in [15, 16]. All background samples have an equivalent luminosity of at least ten times the data collected at each energy.

The contribution to the background from two-fermion final states has been estimated using BHWIDE [17] for the $e^+e^-(\gamma)$ final states and KORALZ [18] for the $\mu^+\mu^-(\gamma)$ and the $\tau^+\tau^-(\gamma)$ states. Multihadronic events, $q\bar{q}(\gamma)$, have been simulated using PYTHIA [19].

For the two-photon background, the PYTHIA [19], PHOJET [20] and HERWIG [21] Monte Carlo generators have been used for $e^+e^-q\bar{q}$ final states and the Vermaseren [22] generator for all $e^+e^-\ell^+\ell^-$ final states. All other four-fermion final states have been simulated with grc4f [23], which takes into account interferences between all four-fermion diagrams.

4 Data Analysis

Pair-produced stable or long-lived massive charged particles would manifest themselves as events with two approximately back-to-back charged tracks. Particles of charge ± 1 are assumed to not interact strongly, hence to not produce hadronic showers. Since they are massive, they do not produce electromagnetic showers either. From these considerations, these events should be very similar to $\mu^+\mu^-$ events, the only difference being the higher mass of the particles.

No assumption is made for the interaction properties of long-lived particles with charge $\pm 2/3$; hence no calorimetric signature is used in the search for such particles, which is described in subsection 4.3.

The events collected by OPAL at $\sqrt{s}$ =130-183 GeV have been required to pass a preselection which rejects events incompatible with the signal topology. The following criteria are applied:

P1 Events are rejected if the total multiplicity of tracks in the central detector and clusters in the ECAL is greater than 18. Cosmic ray events are rejected [24], as well as Bhabha scattering events [25].

P2 Events are required to contain exactly two tracks in the central detector satisfying basic quality criteria[2] and having a momentum $p > 0.1\sqrt{s}$, a momentum transverse to the

[2]The distance between the beam axis and the track at the point of closest approach (PCA) must be less than 1 cm; the z-coordinate of the PCA must be less than 40 cm; the innermost hit of the track measured by the jet chamber must be closer than 75 cm to the beam axis.

beam axis $p_t > 0.025\sqrt{s}$, polar angle satisfying $|\cos\theta| < 0.97$ and at least 20 CJ hits usable for $\mathrm{d}E/\mathrm{d}x$ measurement. The two selected tracks are required to have opposite electric charge.

P3 To reduce background from two-photon interactions, the acoplanarity angle[3] between the two tracks is required to be $\phi_{\mathrm{acop}} < 20^\circ$ and the total visible energy[4] of the event is required to be $E_{\mathrm{vis}} > 0.2\sqrt{s}$.

P4 To reduce background from events with initial state radiation, events containing an isolated ECAL cluster with an energy greater than 5 GeV are rejected. Isolation is defined as an angular separation of more than 15° from the closest charged track.

P5 It is required that $\frac{E_1}{p_1} + \frac{E_2}{p_2} < 0.2$, where $E_{1,2}$ denotes the energies of the ECAL clusters associated to the two selected tracks, to further reduce the contribution from Bhabha scattering events. Moreover, in a cone of 10° half-opening angle around each of the two selected tracks, no other tracks with $p > 0.5$ GeV and no unassociated clusters with $E > 3$ GeV should be found.

After these preselection criteria, the background is dominated by $\mathrm{e^+e^-} \to \mu^+\mu^-$ events, with a small contribution from $\mathrm{e^+e^-} \to \tau^+\tau^-$ and two-photon $\mathrm{e^+e^-}\mu^+\mu^-$ events. The effect of these preselection cuts on the samples at $\sqrt{s} = 183$ GeV is shown in Table 1.

4.1 Search for particles with charge ± 1

Two complementary methods are adopted, depending on the mass m_{X} of the signal particle. In the high-mass ($m_{\mathrm{X}} > 0.36\sqrt{s}$) and low-mass ($m_{\mathrm{X}} < 0.27\sqrt{s}$) regions, the $\mathrm{d}E/\mathrm{d}x$ measurement is used to distinguish the signal from the background. The preselected events are retained if they satisfy the following requirements on $\mathrm{d}E/\mathrm{d}x$:

A1 Both high-momentum tracks must have either $\mathrm{d}E/\mathrm{d}x > 11$ keV/cm or $\mathrm{d}E/\mathrm{d}x < 9$ keV/cm.

A2 The probability that either of the two $\mathrm{d}E/\mathrm{d}x$ measurements originates from one of the standard particles (e, μ, π, p, K) must be less than 10%.

After this selection (**A1**-**A2**), no candidate survives in any of the data sets. The total background is estimated to be 0.03 events at $\sqrt{s} = 130 - 136$ GeV and less than 10^{-2} events at any other energy (see Tables 1, 3).

A complementary analysis is used for masses in the intermediate mass range ($0.27 < m_{\mathrm{X}}/\sqrt{s} < 0.36$), where the $\mathrm{d}E/\mathrm{d}x$ measurement does not provide adequate separation between the signal and the di-lepton background. In events of the type $\mathrm{e^+e^-} \to \mathrm{X^+X^-}$, since $m_{\mathrm{X}} > m_{\mathrm{Z}}/2$ is assumed, initial state radiation is suppressed. Hence, each particle should have an energy close to the beam energy and m_{X} can be estimated for each track as $\widehat{m}_{\mathrm{X}} = \sqrt{s/4 - p^2}$. However, for SM events with two tracks and missing energy (e.g., events with neutrinos, with

[3]The acoplanarity angle, ϕ_{acop}, is defined as 180° minus the angle between the two tracks in the $r-\phi$ plane.

[4]The visible energy, the visible mass and the total transverse momentum of the event are calculated using the method described in [26].

initial state radiation or two-photon interactions), a large overestimate of $\widehat{m}_{\rm X}$ could occur, providing a high background in the accepted mass range. The following selection criteria are designed to reject these backgrounds.

B1 To reject background events with two tracks and neutrinos, the acoplanarity angle of the two tracks is required to be $\phi_{\rm acop} < 1^\circ$.

B2 To reduce the background from two-photon interactions and radiative events, the total visible energy of the event is required to be $E_{\rm vis} > 0.6\sqrt{s}$ and the total momentum along the beam direction is required to be $|p_z^{tot}| < 0.2\sqrt{s}$.

B3 The polar angle of the missing momentum vector must satisfy $|\cos\theta_{miss}| < 0.8$. The total energies measured in the forward detectors (FD, SW, GC) must satisfy: $E_{\rm FD} < 5$ GeV, $E_{\rm SW} < 5$ GeV, $E_{\rm GC} < 5$ GeV. The total energy deposited in the HCAL is required to be less than 15 GeV. The last two requirements introduce relative inefficiencies of at most 3.2% and less than 1%, respectively, due to electronic noise in these detectors; the final efficiencies are corrected by these factors.

B4 Both selected tracks are required to be at least 0.5° away from the CJ anode planes in the $r-\phi$ projection, to avoid momentum mismeasurements.

At this stage the background is mainly due to $\mu^+\mu^-$ events with a smaller contribution from $\tau^+\tau^-$ events where both τ's decay into muons. The intermediate-mass signal is then selected by requiring that:

B5 For both tracks, $\widehat{m}_{\rm X}^2 > (0.27\sqrt{s})^2$. At $\sqrt{s}$=130-136, 161 GeV this cut is not stringent enough, therefore it is required that $\widehat{m}_{\rm X}^2 > (45\ {\rm GeV})^2$. Figure 2(b) shows the distribution of $\widehat{m}_{\rm X}^2$ for both selected tracks, after cut **B4** at $\sqrt{s} = 183$ GeV.

The effect of cuts **B1-B5** for data and simulated events can be seen in Table 1.

An event is selected as a candidate if it satisfies either of the two sets of selection criteria (**A1-A2**) or (**B1-B5**), following the preselections (**P1-P5**). The overall detection efficiency for spin-0 particles is shown in Figure 2(a), as a function of $m_{\rm X}$, for $\sqrt{s} = 183$ GeV. It exceeds 37% even in the mass interval where the ${\rm d}E/{\rm d}x$-based selection is inefficient. At lower centre-of-mass energies the efficiencies have similar values and behaviours. For spin-1/2 particles, the efficiencies are 2-9% lower due to the different angular distribution of the tracks.

After this selection one candidate survives in the $\sqrt{s} = 161$ GeV data set while no candidates are found in the other data samples. The expected backgrounds at 130-136, 161, 172, 183 GeV energies are 0.46, 0.22, 0.31 and 1.01 events, respectively (see Table 3).

The candidate at $\sqrt{s} = 161$ GeV has selected tracks with momenta $p_1 = (51.8 \pm 3.8)$ GeV and $p_2 = (46.7 \pm 2.9)$ GeV, leading to estimated masses of (61.6 ± 3.2) GeV and (65.6 ± 2.1) GeV, respectively. A possible interpretation for this event in the SM is a $\tau^+\tau^-$ event where both τ's decay into μ's.

Cuts	Data	Background Simulation						Signal MC (%)		
		Total	e^+e^-	$\mu^+\mu^-$	$\tau^+\tau^-$	$e^+e^-\ell^+\ell^-$	Others	ϵ_{45}	ϵ_{55}	ϵ_{80}
P1–2	1595	1517.04	806.97	378.71	90.58	147.05	93.73	97.0	97.5	97.7
P3–4	1186	1158.97	636.45	309.29	66.48	109.11	37.63	92.7	93.1	95.8
P5	369	357.11	0.00	288.82	5.07	56.53	6.70	92.5	92.8	95.4
A1,A2	0	0.00	0.00	0.00	0.00	0.00	0.00	84.0	7.5	95.4
B1	297	284.40	0.00	247.73	2.55	32.30	1.81	88.8	90.2	93.0
B2–4	88	92.61	0.00	92.30	0.25	0.00	0.06	61.1	61.4	0.2
B5	0	1.01	0.00	0.85	0.15	0.00	0.01	8.7	32.0	0.0
Comb.	0	1.01	0.00	0.85	0.15	0.00	0.01	84.1	37.5	95.4

Table 1: *The numbers of events remaining after each cut for data collected at $\sqrt{s} = 183$ GeV and for various Monte Carlo background processes normalised to the integrated luminosity of the data ("*Others*" refers to $e^+e^- \to q\bar{q}$, and $e^+e^- \to$ four-fermion processes). In the last three columns the efficiencies for $\tilde{\ell}^{\pm}$ are given (in percent) for $m_X = 45, 55, 80$ GeV. The last line gives the results after combining the two analyses described in the text. The relative rate of data and backgrounds and the composition of the background at lower energies is similar to this case.*

4.2 Systematic uncertainties

The main systematic errors affecting the signal detection efficiencies are listed below and their values are summarised in Table 2. These are: the statistical error from the Monte Carlo samples, the uncertainty due to the linear interpolation of the efficiencies, the evaluation of the integrated luminosity [27], the measurement of $\phi_{\rm acop}$ and the measurement of $E_{\rm vis}$ and $p_z^{\rm tot}$. The uncertainty due to the $\mathrm{d}E/\mathrm{d}x$ measurement (cuts **A1** and **A2**) is estimated as follows: for each Monte Carlo signal event, if both tracks have $\mathrm{d}E/\mathrm{d}x > 11$ keV/cm ($\mathrm{d}E/\mathrm{d}x < 9$ keV/cm), both $\mathrm{d}E/\mathrm{d}x$ values are decreased (increased) by their errors, then the selection cuts are applied to the modified event. The resulting efficiency is therefore lower; the variation in the efficiency is taken as the systematic error. The uncertainty due to the momentum measurement (cut **B5**) is estimated in the same way, but instead of varying the $\mathrm{d}E/\mathrm{d}x$ values, both track momenta are increased by their errors. Again, the resulting decrease in efficiency is taken as the systematic error. The uncertainty due to cut **B5** is estimated to be at most 30% in the intermediate mass region, where it dominates all the systematic effects.

The systematic errors are assumed to be independent, and the total systematic error is calculated as the quadratic sum of the individual errors.

The uncertainty on the background arises essentially from the cuts **A1, A2** and **B5** and is studied in the same way as described above. At $\sqrt{s} = 183$ GeV the uncertainty on the background is $\pm$ 0.69 events. In computing the results, no background subtraction is performed.

4.3 Search for particles with charge $\pm 2/3$

The search for stable and long-lived massive particles with charge $\pm 2/3$ has been performed without assumptions for the interaction properties of such particles. Therefore, requirements on energy deposits in the calorimeters are not applied. The selection is based on $\mathrm{d}E/\mathrm{d}x$ information only. The applied cuts are **P1** through **P4**, followed by **A1** and **A2**.

Quantity	Systematic uncertainty (%)	
	($m_{\rm X}/\sqrt{s} < 0.27$ or $m_{\rm X}/\sqrt{s} > 0.36$)	($0.27 < m_{\rm X}/\sqrt{s} < 0.36$)
MC statistics	0.9-1.6	
Luminosity	0.5-0.9	
$\phi_{\rm acop}$	0.1	
$E_{\rm vis}$, p_z^{tot}	0.5-0.9	
Interpolation	2.0	5.0
$\mathrm{d}E/\mathrm{d}x$	0.0-1.8	1.8-8.9
$\widehat{\mathrm{m}}_{\rm X}$	0.0-1.7	1.7-30.0
Total	2.1-3.5	5.7-30.0

Table 2: *Relative systematic uncertainties associated with the various quantities used. The systematic errors vary slightly with centre-of-mass energy, but strongly with $m_{\rm X}$. The uncertainty in the $\widehat{m}_{\rm X}$ determination dominates in the intermediate mass region but has a small effect in the mass regions where the $\mathrm{d}E/\mathrm{d}x$-based selection is efficient.*

The ionization energy loss $\mathrm{d}E/\mathrm{d}x$ scales roughly as $(Q/e)^2$; hence particles having $|Q/e| = 2/3$ would generally have $\mathrm{d}E/\mathrm{d}x$ values smaller than those of charge ± 1 particle tracks. For masses $m_{\rm X} < 0.41\sqrt{s}$ (e.g., at $\sqrt{s} = 183$ GeV, $m_{\rm X} = 75$ GeV, one has $p = 79$ GeV and $\mathrm{d}E/\mathrm{d}x = 8$ keV/cm) or $m_{\rm X} > 0.44\sqrt{s}$ (e.g., at $\sqrt{s} = 183$ GeV, $m_{\rm X} = 82$ GeV, one has $p = 61$ GeV and $\mathrm{d}E/\mathrm{d}x = 13$ keV/cm), the $\mathrm{d}E/\mathrm{d}x$ for the two tracks of the signal events would be well separated from that of SM di-lepton events, as can be seen from Figure 1. The narrow intermediate region is not covered by any kinematical analysis. However, the efficiency of selections **A1**-**A2** remains larger than 20%, because the small variation of track momenta due to initial state radiation can yield a variation of $\mathrm{d}E/\mathrm{d}x$ which is larger than the excluded range.

After this selection, one candidate remains in the data sample at $\sqrt{s} = 183$ GeV, and no candidates are left in any of the other data sets. The background at $\sqrt{s} = 183$ GeV is estimated to be less than 0.3 events; the total background, summed over all energies, is estimated to be less than 0.45 events, as shown in Table 3. The two tracks of the candidate event have $\mathrm{d}E/\mathrm{d}x$ values of 11.06 ± 0.35 keV/cm and 11.06 ± 0.34 keV/cm, and momenta (70.9 ± 7.0) GeV and (64.7±6.6) GeV, yielding estimated masses of (93.4±9.6) GeV and (88.0±9.8) GeV, respectively (the particle mass is evaluated from the momentum and the estimate of $\beta\gamma$ obtained from the $\mathrm{d}E/\mathrm{d}x$ measurement, assuming $|Q/e|$=2/3). However in this event the mismatch in polar angle between the two selected tracks and the ECAL clusters gives evidence of a reconstruction error of both tracks. This effect is described by the OPAL detector simulation program and would explain an overestimate of the $\mathrm{d}E/\mathrm{d}x$ values by affecting the path length.

The systematic uncertainties on the selection efficiencies are estimated as described in the previous section and they are similar in size.

5 Results

The numbers of candidates found in the search for particles with charge $|Q/e|$=1 and $|Q/e|$=2/3 are summarised in Table 3, together with the expected backgrounds. The data show no excess above the expected background from Standard Model processes. Therefore model-independent

cross-section upper limits have been computed for the pair-production of massive charged long-lived particles.

$\sqrt{s}$ (GeV)	Lumi. (pb^{-1})	$\lvert Q/e\rvert = 1$ search						$\lvert Q/e\rvert = 2/3$ search	
		candidates			background			cand.	back.
		$\mathrm{d}E/\mathrm{d}x$	kin.	comb.	$\mathrm{d}E/\mathrm{d}x$	kin.	comb.		
130-136	11.0	0	0	0	0.03	0.42	0.46	0	<0.08
161	10.1	0	1	1	<0.005	0.22	0.22	0	<0.02
172	10.3	0	0	0	<0.005	0.31	0.31	0	<0.07
183	58.1	0	0	0	<0.005	1.01	1.01	1	<0.27
Total	89.5	0	1	1	0.03	1.96	2.00	1	<0.44

Table 3: *The number of candidate events and the expected background at all energies, for the search for $|Q/e| = 1$ and 2/3 particles. For $|Q/e| = 1$, the result of both the $\mathrm{d}E/\mathrm{d}x$-based and the kinematic selections are shown separately and then combined. In the second column, the integrated luminosity is given for each energy.*

All data collected so far at energies above the Z^0 peak ($\sqrt{s} = 130 - 183$ GeV) have been combined, assuming s-channel production and therefore an energy dependence of the cross-section of β^3/s for spin-0 particles and $\frac{\beta}{s}(1 - \frac{\beta^2}{3})$ for spin-1/2 particles, where $\beta = p/E \simeq \sqrt{1 - 4m_{\mathrm{X}}^2/s}$.

For the production of particles of charge ± 1, the candidate event at $\sqrt{s} = 161$ GeV has been taken into account, assuming a mass of (64.4 ± 1.8) GeV, equal to the weighted average of the two measured masses, mentioned in Section 4.1. Similarly, for particles of charge $\pm 2/3$, the candidate event at $\sqrt{s} = 183$ GeV is included with a mass of (90.7 ± 6.9) GeV. In evaluating upper limits, the candidates are counted in mass intervals centred on their central values and $\pm 2\sigma$ wide. The total systematic error is incorporated into the limits, following the prescription of Ref. [28]. No background subtraction is performed.

In Figure 3, the 95% CL upper limit on the cross-section at $\sqrt{s} = 183$ GeV is shown for spin-0 particles. The 95% CL upper limit on the pair-production cross-section varies from 0.05 to 0.1 pb in the mass range $45 < m_{\mathrm{X}} < 89.5$ GeV. The cross-section limits are compared with the predicted cross-sections for pair-production of right- and left-handed smuons and staus. For these two slepton species, the production cross-section does not depend on the MSSM parameters but only on the slepton mass. The 95% CL lower limits on the mass of right- and left-handed smuons and staus of 82.5 GeV and 83.5 GeV, respectively, are derived, as shown in Figure 3.

Figure 4(a) shows the 95% CL upper limit on the cross-section at $\sqrt{s} = 183$ GeV for spin-1/2 particles; the limit varies from 0.05 to 0.19 pb in the mass range $45 < m_{\mathrm{X}} < 89.5$ GeV. This limit is compared with the predicted cross-sections for chargino production and heavy charged lepton production. The MSSM parameters have been chosen to minimise the predicted chargino cross-section at every chargino mass value (assuming a heavy sneutrino, $m_{\tilde{\nu}} > 500$ GeV), without any restriction on the mass of the lightest neutralino. Therefore a 95% CL lower limit on the masses of long-lived charginos is derived at 89.5 GeV for every choice of the MSSM parameters. The 95% CL lower limit on the heavy charged lepton mass is 89.5 GeV.

Figure 4(b) shows the 95% CL upper limit on the cross-section at $\sqrt{s} = 183$ GeV for spin-1/2 particles of charge $\pm 2/3$; the limit varies between 0.05 to 0.2 pb in the mass range $45 <$

$m_{\mathrm{X}} < 89.5$ GeV. For spin-0 leptoquarks the cross-section upper limits would be slightly better than those calculated from spin-1/2 particles. These limits can be compared with leptoquarks and deconfined quarks models which provide cross-section predictions.

The results obtained are valid for particles with a lifetime longer than 10^{-6} s. This is calculated in the worst case, e.g. the heaviest (and therefore slowest) particles excluded by this search, requiring that the decay probability of these particles at a flight distance larger than 3.0 m is greater than 95%. For lower mass values the results are also valid for shorter lifetimes.

6 Summary and Conclusions

A search has been performed for pair-production of stable and long-lived massive particles with charge $|Q/e| = 1$ or 2/3. The primary tool used in this search is the precise $\mathrm{d}E/\mathrm{d}x$ measurement provided by the OPAL jet chamber. No evidence for the production of heavy particles with masses in the range of 45 to 89.5 GeV was observed. For s-channel production, the upper limits on the cross-section vary between 0.05 and 0.19 pb in the range of masses explored for particles of charge ± 1. Within the framework of the MSSM, lower mass limits on the the right- (left-) handed smuons and staus of 82.5 GeV (83.5 GeV) have been obtained. Heavy long-lived charged leptons and long-lived charginos with masses smaller than 89.5 GeV are excluded. For particles with charge $\pm 2/3$ the upper limits on the production cross-section vary between 0.05 and 0.2 pb in the range of masses explored. The above limits are valid at the 95% CL for particles with lifetimes longer than 10^{-6} s.

Acknowledgements

We particularly wish to thank the SL Division for the efficient operation of the LEP accelerator at all energies and for their continuing close cooperation with our experimental group. We thank our colleagues from CEA, DAPNIA/SPP, CE-Saclay for their efforts over the years on the time-of-flight and trigger systems which we continue to use. In addition to the support staff at our own institutions we are pleased to acknowledge the
Department of Energy, USA,
National Science Foundation, USA,
Particle Physics and Astronomy Research Council, UK,
Natural Sciences and Engineering Research Council, Canada,
Israel Science Foundation, administered by the Israel Academy of Science and Humanities,
Minerva Gesellschaft,
Benoziyo Center for High Energy Physics,
Japanese Ministry of Education, Science and Culture (the Monbusho) and a grant under the Monbusho International Science Research Program,
German Israeli Bi-national Science Foundation (GIF),
Bundesministerium für Bildung, Wissenschaft, Forschung und Technologie, Germany,
National Research Council of Canada,
Research Corporation, USA,
Hungarian Foundation for Scientific Research, OTKA T-016660, T023793 and OTKA F-023259.

References

[1] H. P. Nilles, Phys. Rep. 110 (1984) 1;
H. E. Haber and G. L. Kane, Phys. Rep. 117 (1985) 75.

[2] S. Dimopoulos, S. Thomas and J. D. Wells, Nucl. Phys. B488 (1997) 39;
S. Ambrosanio, G. D. Kribs and S. P. Martin, Phys. Rev. D56 (1997) 1761;
G. F. Giudice and R. Rattazzi, *"Theories with Gauge-Mediated Supersymmetry Breaking"*, CERN-TH/97-380, hep-ph/9801271 (1997).

[3] H. Dreiner, *"An Introduction to Explicit R-parity Violation"*, hep-ph/9707435.

[4] E. Nardi, E. Roulet and D. Tommasini, Phys. Lett. B344 (1995) 225.

[5] J. L. Hewett and T. G. Rizzo, Phys. Rev. D56 (1997) 5709.

[6] A. de Rujula, R. C. Giles and R. L. Jaffe, Phys. Rev. D17 (1978) 285;
R. Slansky, T. Goldman and G. L. Shaw, Phys. Rev. Lett. 47 (1981) 887;
D. G. Caldi and S. Nussimov, Phys. Rev. D28 (1983) 3138.

[7] ALEPH Collab., D. Decamp *et al.*, Phys. Lett. B303 (1993) 198;
DELPHI Collab., P. Abreu *et al.*, Phys. Lett. B247 (1990) 157;
OPAL Collab., K. Ahmet *et al.*, Phys. Lett. B252 (1990) 290;
OPAL Collab., R. Akers *et al.*, Z. Phys. C67 (1995) 203.

[8] ALEPH Collab., R. Barate *et al.*, Phys. Lett. B405 (1997) 379;
DELPHI Collab., P. Abreu *et al.*, Phys. Lett. B396 (1997) 315.

[9] OPAL Collab., K. Ahmet *et al.*, Nucl. Instr. Meth. A305 (1991) 275;
P. P. Allport *et al.*, Nucl. Instr. Meth. A324 (1993) 34;
P. P. Allport *et al.*, Nucl. Instr. Meth. A346 (1994) 476.

[10] M. Hauschild *et al.*, Nucl. Instr. Meth. A314 (1992) 74;
M. Hauschild, Nucl. Instr. Meth. A379 (1996) 436.

[11] B.E. Anderson *et al.*, IEEE Transactions on Nuclear Science 41 (1994) 845.

[12] J. Allison *et al.*, Nucl. Instr. Meth. A317 (1992) 47.

[13] S. Katsanevas and S. Melachroinos, in *"Physics at LEP2"*, eds. G. Altarelli, T. Sjöstrand and F. Zwirner, CERN 96-01, vol. 2, p. 328 (1996).

[14] R. Tafirout, *"EXOTIC, A Heavy Fermion and Excited Fermion Monte Carlo Generator for* e^+e^- *Physics"*, private communication.

[15] OPAL Collab., G. Alexander *et al.*, Z. Phys. C73 (1997) 189.

[16] OPAL Collab., K. Ackerstaff *et al.*, Phys. Lett. B396 (1997) 301.

[17] S. Jadach, W. Placzek and B.F.L. Ward, UTHEP/95-1001 (unpublished);
S. Jadach *et al.*, in *"Physics at LEP2"*, eds. G. Altarelli, T. Sjöstrand and F. Zwirner, CERN 96–01, vol.2, p. 229 (1996);
S. Jadach, W. Placzek and B.F.L. Ward, Phys. Lett. B390 (1997) 298.

[18] S. Jadach, B.F.L. Ward and Z. Wąs, Comp. Phys. Comm. 79 (1994) 503.

[19] T. Sjöstrand and M. Bengtsson, Comp. Phys. Comm. 43 (1987) 367;
"PYTHIA 5.7 and JETSET 7.4, Physics and Manual", CERN-TH. 7112/93 (revised August 1995);
T. Sjöstrand, Comp. Phys. Comm. 82 (1994) 74.

[20] R. Engel and J. Ranft, Phys. Rev. D54 (1996) 4244;
R. Engel, Z. Phys. C66 (1995) 203.

[21] G. Marchesini *et al.*, Comp. Phys. Comm. 67 (1992) 465.

[22] R. Bhattacharya, J. Smith and G. Grammer, Phys. Rev. D15 (1977) 3267;
J. Smith, J.A.M. Vermaseren and G. Grammer, Phys. Rev. D15 (1977) 3280.

[23] J.Fujimoto *et al.*, Comp. Phys. Comm. 100 (1997) 128.

[24] OPAL Collab., R. Akers *et al.*, Z. Phys. C61 (1994) 19.

[25] S. Robins, *"A Study of Bhabha Scattering at LEP"*, Ph.D. Thesis (1992), Queen Mary and Westfield College (unpublished).

[26] OPAL Collab., M.Z. Akrawy *et al.*, Phys. Lett. B253 (1991) 511.

[27] OPAL Collab., K.Ackerstaff *et al.*, Phys. Lett. B391 (1997) 221.

[28] R. D. Cousins and V. L. Highland, Nucl. Instr. Meth. A320 (1992) 331.

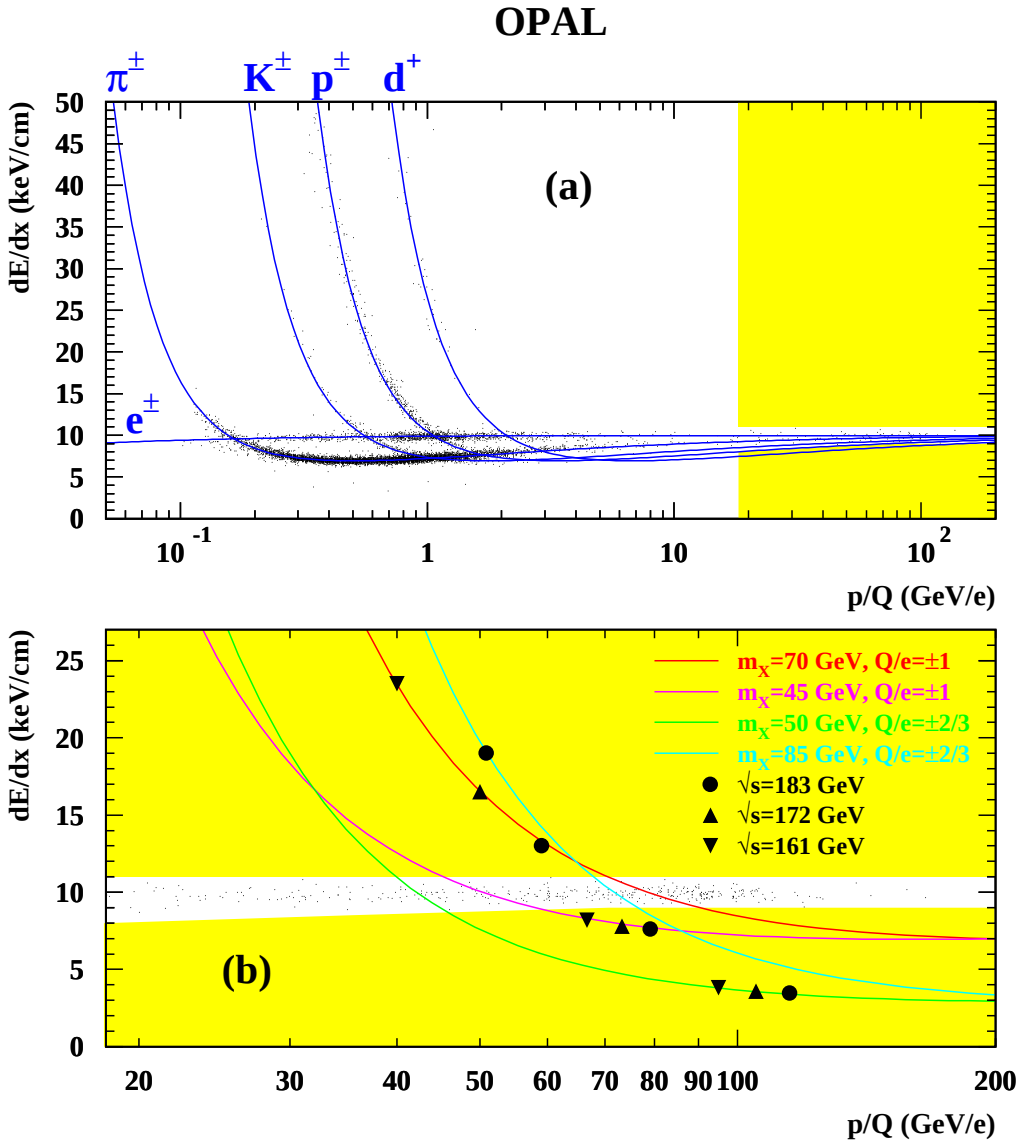

Figure 1: *(a) The distribution of the ionization energy loss,* $\mathrm{d}E/\mathrm{d}x$*, as a function of the apparent momentum* p/Q *for data collected at* $\sqrt{s} = 183$ *GeV. The two hatched regions are the search regions at* $\sqrt{s} = 183$ *GeV. The momentum lower limit is defined by the preselection cut* $p > 0.1\sqrt{s}$*. A cutoff of* $p_t > 0.1$ *GeV is made to reject low momentum tracks curling in the jet chamber volume.*
(b) Expanded view of the search regions. The theoretical curves for heavy long-lived particles are shown. In $\mathrm{e^+e^-} \to \mathrm{X^+X^-}$ *events, the momentum of the* $\mathrm{X^\pm}$ *particles of a given mass is fixed by* $\sqrt{s}$*. For* $|Q/e| = 2/3$*,* $m_\mathrm{X} = 85$ *GeV only the position at* $\sqrt{s} = 183$ *GeV is visible, while at* $\sqrt{s} = 172$ *GeV the* $\mathrm{d}E/\mathrm{d}x$ *value lies outside the plot;* $\sqrt{s} = 161$ *GeV is below the pair-production threshold for this mass.*

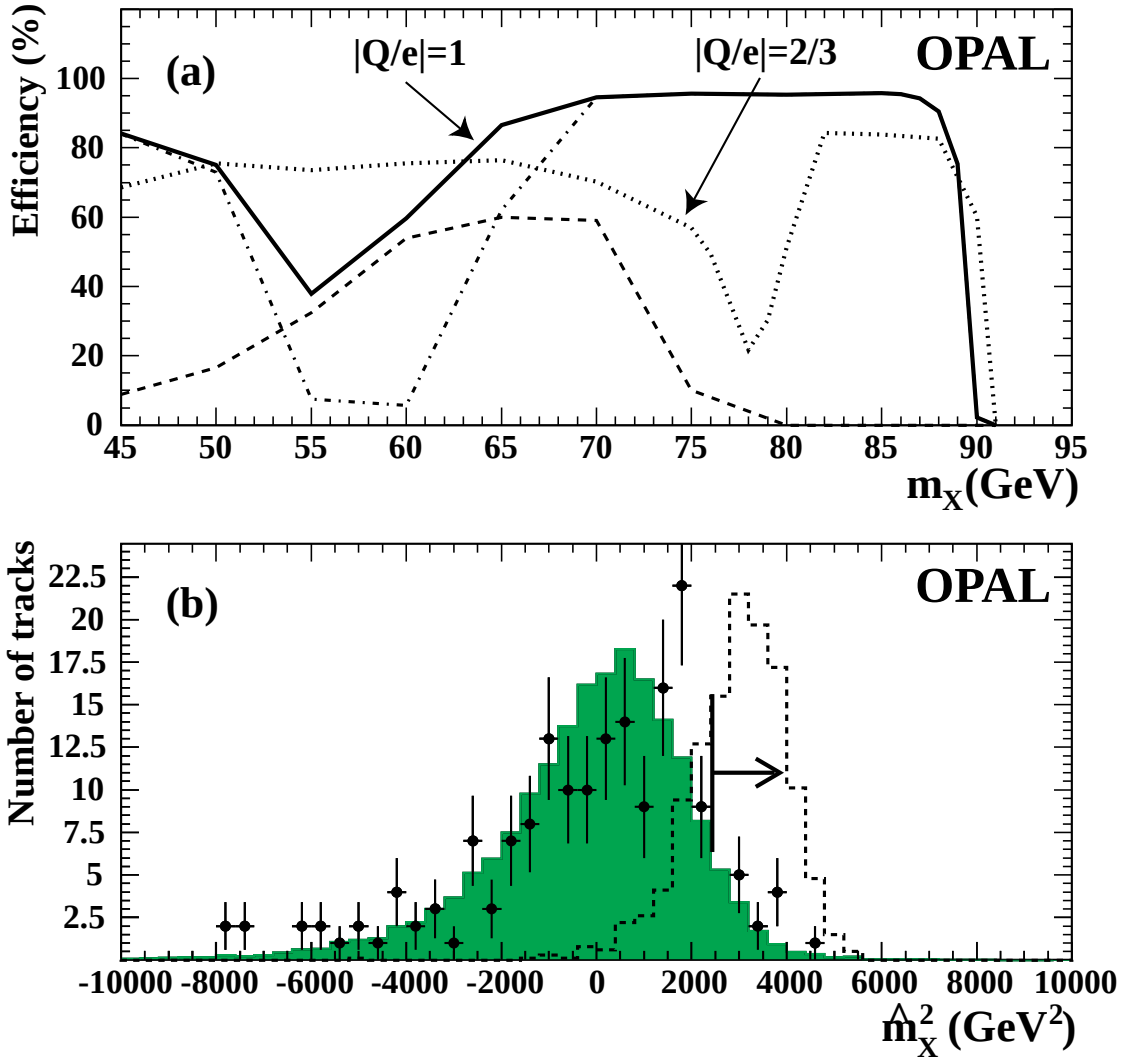

Figure 2: *(a) Selection efficiency as a function of the mass m_X for $|Q/e| = 1$ and 2/3 particles, at $\sqrt{s} = 183$ GeV. The dashed-dotted and dashed lines represent the efficiency of the $\mathrm{d}E/\mathrm{d}x$-based and kinematic selections, respectively, in the case of the spin-0 particles of charge ± 1. The solid line refers to the combined selection. The dotted line represents the overall efficiency of the search for spin-1/2 particles of charge $\pm 2/3$.*
(b) The distribution of the $\widehat{m}_X^2$, after cut **B4**, *for data collected at $\sqrt{s} = 183$ GeV (points with error bars), for all simulated backgrounds (grey histogram) and for a simulated signal (dashed line) with m_X=55 GeV. The signal histogram is arbitrarily normalised. The cut* **B5** *is indicated by the arrow pointing to the accepted region. No event is selected when both selected tracks are required to pass this cut.*

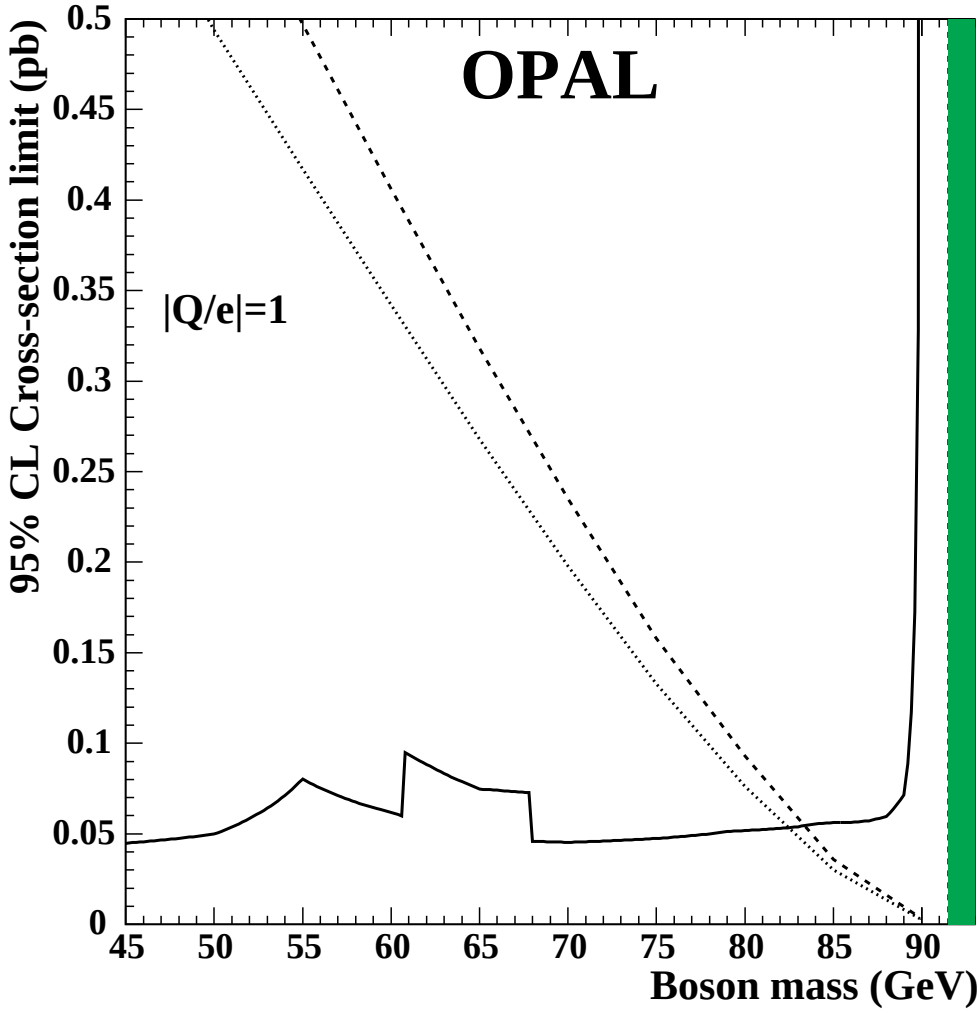

Figure 3: *Model-independent 95% CL upper limits on the pair-production cross-section of spin-0 heavy long-lived particles of charge ±1 as a function of their mass (solid line). In calculating the upper limit, the candidate is considered as described in the text. The MSSM predicted cross-sections for right-handed (dotted line) and left-handed (dashed line) smuons and staus are also shown. The 95% CL lower limits on the masses of these sleptons are at the crossing point between the experimental and theoretical curves. The grey region is kinematically inaccessible.*

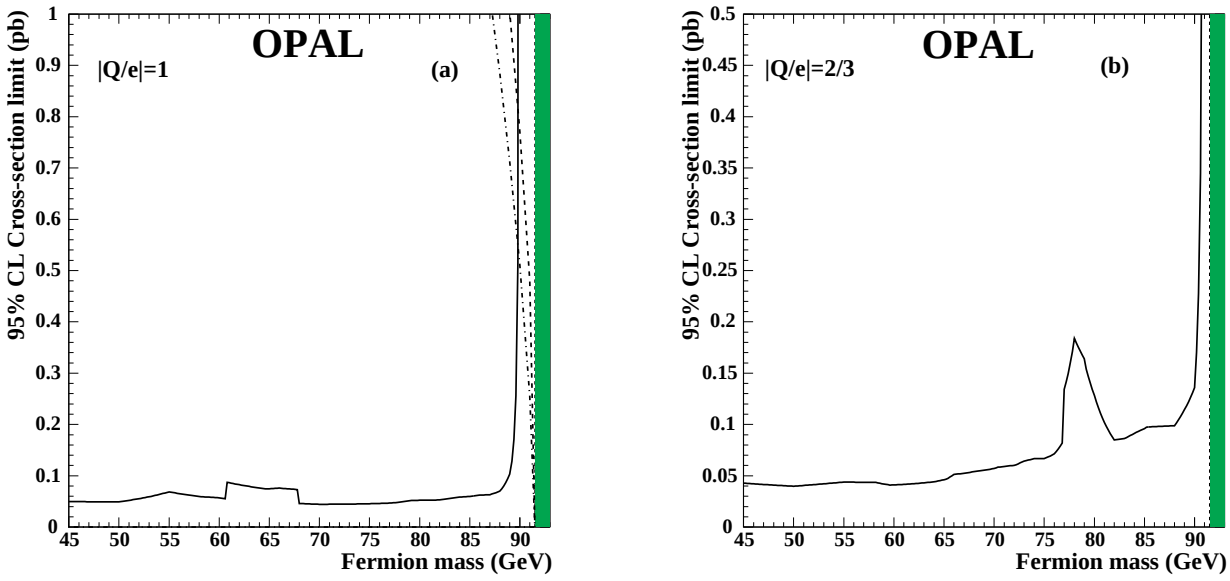

Figure 4: *(a) Model-independent 95% CL upper limits on the pair-production cross-section of spin-1/2 heavy long-lived particles of charge ±1 as a function of their mass (solid line). In calculating the upper limit, the candidate is considered as described in the text. The MSSM predicted cross-sections for charginos (dashed line) and heavy leptons (dashed-dotted line) are also shown. The 95% CL lower limits on the masses of these particles are at the crossing point between the experimental and theoretical curves. (b) Model-independent 95% CL upper limits on the pair-production cross-section of spin-1/2 heavy particles of charge ±2/3 as a function of their mass (solid line). In both plots the grey region is kinematically inaccessible.*